Fractals, Vol. 17, No. 1 (2009) 1–14

World Scientific
www.worldscientific.com

Articles

A PRIMER OF NEGATIVE TEST DIMENSIONS AND DEGREES OF EMPTINESS FOR LATENT SETS

BENOIT B. MANDELBROT and MICHAEL FRAME*
Mathematics Department, Yale University
10 Hillhouse Ave., P. O. Box 208283
New Haven, CT, 06520-8283, USA
**michael.frame@yale.edu*

Received January 20, 2008
Accepted July 22, 2008

Abstract

Applied blindly, the formula for the dimension of the intersection can give negative results. Extending Minkowski's definition of the dimension by ϵ-neighborhoods to ϵ-pseudo-neighborhoods, that is, replacing $(A \cap B)_\epsilon$ with $A_\epsilon \cap B_\epsilon$, we introduce the notion of negative dimensions through several examples of random fractal constructions.

Keywords: Negative Dimension; Pseudo-neighborhoods; Birth and Death Processing; Super-sampling.

1. INTRODUCTION

Fractal geometry has made a number of facts about generalized notions of dimension useful in the sciences — commonplace even, and known to general audiences. Dimension allows several distinct interpretations and some sets have important properties best described by non-integer values of dimension. At first blush, this contradicts the analytic

*Corresponding author.

geometry of Descartes, where the term "(Euclidean) dimension" D_E refers to the number of independent directions occupied by an object. This common interpretation is important because it generalizes our experience with the physical world, but dimension has many other meanings.

A key feature of fractal geometry is that it uses dimension to give quantitative measures to central features common to several natural notions with which experimental science has long struggled; they concern roughness, irregularity, and brokenness. These measurements include the similarity dimension D_s (recalled in Sec. 4), the box-counting dimenson D_b of Minkowski and Bouligand (recalled in Sec. 5), the Hausdorff dimension (see Ch. 2 of Ref. 1), and the packing dimension D_p (not used in this analysis, but useful in many contexts, see Ch. 3 of Ref. 1).

This paper presents a simple exposition and illustrative examples of the next step away from Euclidean geometry — namely, the move from controllable degrees of roughness to degress of emptiness achieved by different methods of successive erasure. This direction may appear to be a form of much ado about nothing, but is not. It was first explored in Refs. 2 to 7, and made rigorous in Sec. 1.3.3 and Ch. 3 of Ref. 8.

A central role is played by the generalized concept of *test dimension*. The original notion of dimension refers to a set, but in some cases and for some calculations, dimension refers to a process generating the set. Even when no such process is involved, Minkowski[9] showed that an auxiliary sequence of preasymptotic ϵ-neighborhoods may greatly help to understand the underlying mathematics of a process or a geometric object. New evidence now exists that it may also have a physical reality — one that demands and deserves a careful mathematical treatment — which we shall attempt to provide.

As background, the simplest self-similar fractal set consists of N copies of itself, each scaled by a factor r. The Sierpinski gasket, shown on the right side of Fig. 1, consists of $N = 3$ copies of itself, each scaled by $r = 1/2$. The similarity dimension, as given by the familiar formula $D_s = \log(N)/\log(1/r)$, is $\log(3)/\log(2)$ for the gasket. As illustrated in the first three images of Fig. 1, the numbers 3 and 2 describe the *generating process*: replace each copy of the triangle by $N = 3$ copies, each scaled by a factor of $r = 1/2$.

Fig. 1 A process generating the Sierpinski gasket.

In familiar cases such as the gasket, almost all of our understanding of the set is derived from its generating process. When the fractal is random, to the contrary, a negative value of the dimension may play an altogether different role. It may help distinguish between generative algorithms that share the overall feature that the generated sets are empty, yet greatly differ in other ways of practical relevance. An image to be kept in mind is the distinction between (a) sequences with a limit in $(0, \infty)$ and (b) sequences converging to 0 or ∞ according to one among infinitely many possible distinct rates. The first and still most significant such distinction arose in the context of the random multifractal measures of turbulence. For example, see all of Ref. 10, Figs. 3 and 4 of Ref. 11, page 570 of Ref. 12, Figs. 24, 33, and 40 of Ref. 13, Sec. 4 of Ref. 14, Fig. 1 of Ref. 15, and Ref. 16. This setting is the topic of the exposition.[17] This paper, however, keeps (mostly) clear of the complexities of multifractal measures. Rather, it deals solely with sets, and presents a simple introduction to negative dimension based on a generalization to random fractal processes of the intersection formula for dimensions.

Quantitative degrees of roughness and emptiness are provided by the notion of *test dimension*, D_t, introduced by the senior author and discussed in Sec. 6. When it is positive, $D_t = D_b$, the box-counting dimension. When it is negative and the set is almost surely empty, D_t measures the degree of emptiness of a *latent set*, a concept that is discussed in Sec. 7. This replaces the universal empty set with a multitude of cases referencing the generative process by which the set became empty. This may seem counterintuitive, but can be measured empirically and already has shown its usefulness, for example in engineering problems,[10,11] involving multifractals, in clusters in statistical physics,[18] and in the intersection of EEG signals.[19] Table 1 is a summary of some of the principal types of dimension. One goal of this paper is to introduce the test dimension, D_t.

For obtaining negative dimensions, the central role of randomness can be seen through a simple illustration. Suppose that each stage of the construction of a random set involves a random number

Table 1 Some Principle Types of Dimension.

D_{top}	Topological	Connectivity
D_E	Euclidean	Cardinality of a basis
D_s	Similarity	Scaling under decomposition
D_h	Hausdorff-Besicovitch	Discontinuity of measure
D_b	Box-counting	Scaling of coverings
D_p	Packing	Scaling of packings
D_t	Test	Roughness/emptiness

N of scaled copies, so that samples of the limiting process create a population of distinct fractals. In this case, the similarity dimension is redefined as $\log(E(N))/\log(1/r)$, where $E(N)$ denotes the expected value of N. If $E(N) > 1$, then for almost all sample limits this expression coincides with the values that other definitions (such as D_b and D_h) assign to the sample limit set.

The paper focuses on the unconventional case when $E(N) < 1$, hence

$$\log(E(N))/\log(1/r) < 0.$$

If so, the construction of the preceding paragraph almost surely produces an empty limit set. Classical dimension theory[20] assigns to the empty set the only negative dimension it allows: $D_{top} = -1$. The universality of this value confirms that, in common mathematical thinking, the empty set is unique: the set consisting of no oranges is identical to the set consisting of no apples.

To avoid possible confusion arising from studying "degrees of emptiness of the empty set," the name *latent set* is assigned to the almost surely empty limits of iterative processes with $E(N) < 1$. Because this refers to samples of random processes, the dimension is called the "test dimension." "Sample dimension" was another possibility; the shorter term is preferable. A goal of this paper is to show that different negative values of D_t distinguish between different latent sets, that is, given almost impossible events negative test dimensions can be used to assign to them different degrees of almost impossibility.

The objects for which the negative test dimension was first developed were not fractal or Euclidean sets, but the multifractal measures that are revealed in the study of turbulence (see Refs. 11 and 21, for example). Negative dimension in the context of multifractal measures is taken up in Ref. 2 and the sequel Ref. 17. It should be noted that a non-geometric negative dimension, unrelated to test dimension or to fractals, goes back at least to Ref. 22.

This extension of dimension into the negative range follows the pattern of negative numbers replacing the unique notion of "being in debt" by multiple notions of "owing some or another amount of money." This requires embedding the positive axis in the real line. Imaginary numbers began as quantities needed to solve all quadratic equations; the later step that gave them a geometric interpretation consisted in embedding the real line in the plane. In roughly parallel fashion, in Sec. 8 we see embedding is a key step for interpreting negative test dimensions.

2. SOME ALGEBRA OF DIMENSIONS OF EUCLIDEAN SETS

The dimensions of ordinary Euclidean sets are nonnegative integers which obey several rules that are rarely stated but are well-known and intuitively plausible, and, under mild conditions, are rigorously provable.

Monotonicity. If $A \subseteq B$, then $\dim(A) \leq \dim(B)$.

Union. Typically, the dimension of the union of two sets is the maximum of the dimensions of the sets: $\dim(A \cup B) = \max\{\dim(A), \dim(B)\}$.

Product. Typically, the dimension of the Cartesian product of two sets is the sum of the dimensions of the sets: $\dim(A \times B) = \dim(A) + \dim(B)$.

Intersection. Typically, the codimension of the intersection of two sets is the sum of the codimensions of the sets: $e - \dim(A \cap B) = (e - \dim(A)) + (e - \dim(B))$, where A and B are subsets of $\mathbb{R}^e$. The intersection rule also is called the *codimension addition rule*. More directly, the rule is

$$\dim(A \cap B) = \dim(A) + \dim(B) - e. \qquad (1)$$

A key fact is that this typical intersection rule suffers exceptions. With dimension as it is usually understood the intersection rule is subject to what will be called a *key caveat*. It is analogous to the very familiar restrictions that used to allow subtraction only if the difference was nonnegative, or square roots only if the radicand was nonnegative.

Key caveat: when the intersection rule yields $\dim(A \cap B) = \delta < 0$, then typically $A \cap B$ is empty.

Does it follow that these negative values of δ are an idle imaginary product of formal manipulation let loose? Or perhaps δ has no reality but can be assigned some redeeming practical value? The terms

"imaginary" and "real" have been choosen to hint at things to come.

Mandelbrot[23] generalized these rules of algebra of dimensions to random fractals, and interpreted negative test dimensions as measures of a *degree of emptiness* (see Sec. 7).

3. THE CODIMENSION ADDITION RULE: EXAMPLES AND A FIRST GLIMPSE OF NEGATIVE-VALUED FORMAL DIMENSIONS

The codimension addition rule is the least-familiar of the four algebra of dimension rules. To illustrate, suppose A and B are planes in $\mathbb{R}^3$. Then by Eq. (1)

$$\dim(A \cap B) = \dim(A) + \dim(B) - 3 = 1 :$$

planes in space typically intersect in a line.

If A is a plane and B is a line in $\mathbb{R}^3$, the analogous calculation yields $\dim(A \cap B) = 0$: in space a plane and a line typically intersect in a point. If A and B are lines in $\mathbb{R}^3$, then $\dim(A \cap B) = -1$: in space two lines typically do not intersect at all, that is, intersect in the empty set.

To construct more examples, note that the intersection rule generalizes to intersections of more than two sets. For instance,

$$\begin{aligned} e - \dim(A \cap B \cap C) \\ = (e - \dim(A)) + (e - \dim(B)) \\ + (e - \dim(C)) \end{aligned}$$

that is,

$$\begin{aligned} \dim(A \cap B \cap C) = \dim(A) + \dim(B) \\ + \dim(C) - 2e \end{aligned} \tag{2}$$

where A, B and C are subsets of $\mathbb{R}^e$. For a standard Euclidean example, three planes in $\mathbb{R}^3$ typically intersect in a point. Figure 2 shows some other examples, all pictures taking place in $\mathbb{R}^3$. The first two are elementary geometry. The others, proceeding through the figure yield increasingly negative dimensions. Very roughly, the more negative the dimension, the more easily the components miss one another. Equation (2) makes clear the central role of the dimension of the ambient space in giving rise to negative dimensions of intersections.

How can the notion of negative dimensions be made precise? Randomness must be injected and the Minkowski approach to dimension must be modified by replacing his notion of ϵ-neighborhood by a notion of ϵ-pseudo-neighborhood. This topic is treated in Sec. 6. First, the (always positive) notions of similarity and box-counting dimensions are reviewed in Secs. 4 and 5.

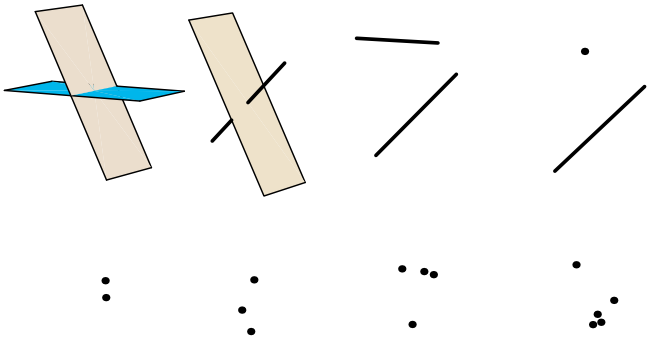

Fig. 2 Left to right, top to bottom: the codimension addition rule gives typical intersections of dimension 1, 0, −1, −2, −3, −6, −9, and −12.

4. THE (ALWAYS POSITIVE) SIMILARITY DIMENSION

For a self-similar set consisting of N pieces, each linearly scaled by the same factor of r, the similarity dimension is defined by

$$D_s = \frac{\log(N)}{\log(1/r)}. \tag{3}$$

For example, the Sierpinski gasket (Fig. 3, left) consists of $N = 3$ pieces, each scaled by a factor of $r = 1/2$, so the similarity dimension of the gasket is $D_s = \log(3)/\log(2)$.

This notion is extended easily to self-similar sets for which different pieces are scaled by different factors. Suppose the set F can be written as $F = F_1 \cup \cdots \cup F_N$ with each F_i a copy of F scaled by a factor r_i, with $0 < r_i < 1$ for each i. To accommodate these different values for r_i, note Eq. (3) can be rewritten as

$$1 = N \cdot r^{D_s} = r^{D_s} + \cdots + r^{D_s}.$$

Generalizing by replacing r with values r_i that need not be equal gives rise to the *Moran equation*:

$$\sum_{i=1}^{N} r_i^D = 1. \tag{4}$$

Since each r_i satisfies $0 < r_i < 1$, analyzing the graph of $f(r) = \sum_i r_i^D$ shows the Moran equation has a unique solution, $D = D_s$. The right side of Fig. 3 shows a self-similar set consisting of three

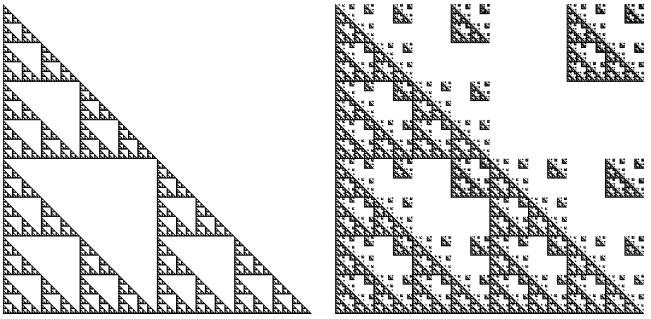

Fig. 3 Left: the Sierpinski gasket, consisting of three pieces scaled by 1/2. Right: a self-similar fractal consisting of three pieces scaled by 1/2 and one piece scaled by 1/4.

pieces scaled by $r_1 = r_2 = r_3 = 1/2$ and one piece scaled by $r_4 = 1/4$. The Moran equation is $3(1/2)^D + (1/4)^D = 1$ and can be rewritten as the quadratic equation $x^2 + 3x - 1 = 0$ in $x = (1/2)^D$. Solving gives $D = \log((-3 + \sqrt{13})/2)/\log(1/2)$.

Under fairly general conditions (for example, Hutchinson's *Open Set condition* of Ref. 24 and Sec. 9.2 of Ref. 1), the similarity dimension equals the Hausdorff-Besicovitch dimension D_H, a quantity of great importance though often difficult to evaluate. While D_H figures heavily in Ref. 17, here we rely on D_B and D_s, except for a brief mention of D_H in Sec. 10.

Before moving on to box-counting dimension, we must mention another generalization by Lapidus and van Frankehhuijsen[25] and their co-workers. This is the notion of *complex dimension*. For example, consider a Cantor set constructed in $[0, 1]$ with gaps $l_1 \geq l_2 \geq l_3 \geq \ldots$. This is called a *fractal string*, $\mathcal{L}$. The geometric zeta function of $\mathcal{L}$ is

$$\zeta_{\mathcal{L}}(s) = \sum_{j=1}^{\infty} l_j^s. \tag{5}$$

The complex dimensions of $\mathcal{L}$ are the poles of $\zeta_{\mathcal{L}}(s)$. If the Cantor set is self-similar with scaling factors $r_1, \ldots, r_N$, then the complex dimensions also are the (complex) solutions ω of

$$r_1^{\omega} + \cdots + r_N^{\omega} = 1 \tag{6}$$

clearly an extension of the Moran Eq. (4).

For a concrete example, consider the standard Cantor middle thirds set. Then the geometric zeta function of Eq. (5) is

$$\left(\frac{1}{3}\right)^s + 2\left(\frac{1}{9}\right)^s + 4\left(\frac{1}{27}\right)^s + \cdots = \frac{(1/3)^s}{1 - 2(1/3)^s}.$$

The poles are simple, and occur at $D = \log_3(2) + i2k\pi/\ln(3)$. Note these values of D also are the solutions of

$$\left(\frac{1}{3}\right)^{\omega} + \left(\frac{1}{3}\right)^{\omega} = 1,$$

Eq. (6) for this example. For many more examples and fascinating interpretations, consult Ref. 25.

5. THE (ALWAYS-POSITIVE) BOX-DIMENSION OF MINKOWSKI-BOULIGAND

The similarity dimension is computed easily, but is defined only for self-similar sets. Among the dimensions defined for more general sets, the box-counting dimension is computed most easily. Denoting by $N(\epsilon)$ the minimum number of boxes of side length ϵ needed to cover A, we seek a power-law scaling of the form

$$N(\epsilon) \sim \epsilon^{-d}. \tag{7}$$

If there is such a scaling, then $D_b = d$ is the *box-counting dimension* of A.

Instead of the power-law formulation, we follow Minkowski's approach. For any subset $A \subset \mathbb{R}^e$, denote by A_ϵ the ϵ-neighborhood (nbhd) of A:

$$A_\epsilon = \{x \in \mathbb{R}^e : \text{dist}(x, z) \leq \epsilon \text{ for some } z \in A\}.$$

Minkowski argued that for a d-dimensional Euclidean set $A \subset \mathbb{R}^e$, $\text{vol}(A_\epsilon)$ scales as ϵ^{e-d}, and Bouligand extended this to the case on non-integer d, but for which dimension d? The correct dimension is the box-counting dimension D_b.

Assuming $vol(A_\epsilon) \sim k\epsilon^{e-d}$ for some constant k, and assuming the approximation gets better for smaller ϵ,

$$D_b(A) = e - \lim_{\epsilon \to 0} \frac{\log(\text{vol}(A_\epsilon))}{\log(\epsilon)} \tag{8}$$

with the understanding that if the limit does not exist, it is replaced with $\overline{\lim}$ and $\underline{\lim}$, obtaining lower and upper box-counting dimensions $\underline{D}_b(A)$ and $\overline{D}_b(A)$. See Proposition 3.2 of Ref. 1 for an accessible development.

Before constructing our first example, we mention that the ϵ-nbhd approach also has been used to great effect in studying fractals in other settings. See Refs. 26 and 27, for example.

Example 5.1. Computing the dimension of the Sierpinski gasket by the approach of Minkowski and Bouligand.

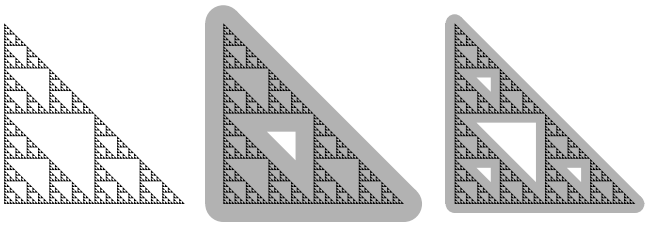

Fig. 4 The gasket and two ϵ-nbhds.

Suppose the altitude and base of the gasket G have length 1. Denote by ϵ_1 the smallest value of ϵ for which G_ϵ has no holes, by ϵ_2 the smallest value of ϵ for which G_ϵ has a single hole, by ϵ_3 the smallest value of ϵ for which G_ϵ has four holes, and so on. Some straightforward geometry gives

$$\epsilon_n = \frac{1}{2^n(2+\sqrt{2})}.$$

To understand the pattern of G_{ϵ_n}, observe that G_{ϵ_1} is the filled-in triangle, together with a band of width ϵ_1, so

$$\text{Area}(G_{\epsilon_1}) = \frac{1}{2} + (2+\sqrt{2})\epsilon_1 + \pi\epsilon_1^2 = \frac{1}{2} + P(\epsilon_1)$$

where $P(\epsilon_1)$ denotes the area of the part of the ϵ_1-nbhd of the gasket perimeter lying outside the perimeter. On the left of Fig. 4 is the gasket; center and right are ϵ-nbhds G_ϵ for $\epsilon_1 > \epsilon > \epsilon_2$ and $\epsilon_2 > \epsilon > \epsilon_3$, resp. Note as $\epsilon \to 0$, in G_ϵ more and more holes arise and existing holes become enlarged.

Next, G_{ϵ_2} is the filled-in triangle with a hole having vertices $(\frac{1}{2},0),(\frac{1}{2},\frac{1}{2})$ and $(0,\frac{1}{2})$, together with a band of width ϵ_2 along the outside and inside edges, leaving a triangular hole with base and altitude $1/2-(1+\sqrt{2})\epsilon_2$. Thus

$$\text{Area}(G_{\epsilon_2}) = \frac{1}{2} + P(\epsilon_2) - \frac{1}{2}\left(\frac{1}{2} - (1+\sqrt{2})\epsilon_2\right)^2.$$

With each successive ϵ_n, more triangular holes open, yielding

$$\text{Area}(G_{\epsilon_n}) = \frac{1}{2} + P(\epsilon_n) - \frac{1}{2}\left(\frac{1}{2} - (1+\sqrt{2})\epsilon_n\right)^2 - \cdots - \frac{1}{2}3^{n-2}\left(\frac{1}{2^{n-1}} - (1+\sqrt{2})\epsilon_n\right)^2.$$

Expanding the squared terms, grouping like powers of ϵ_n, summing the finite geometric series, and simplifying, yields

$$\begin{aligned}\text{Area}(G_{\epsilon_n}) &= P(\epsilon_n) + \frac{1}{2}\left(\frac{3}{4}\right)^{n-1} - (1+\sqrt{2})\epsilon_n\left(1 - \left(\frac{3}{2}\right)^{n-1}\right) \\ &\quad + \frac{1}{4}((1+\sqrt{2})\epsilon_n)^2(1-3^{n-1}) \\ &= \epsilon_n + \left(\pi + \frac{3+2\sqrt{2}}{4}\right)\epsilon_n^2 + \frac{1}{2}\left(\frac{3}{4}\right)^{n-1} \\ &\quad + (1+\sqrt{2})\epsilon_n\left(\frac{3}{2}\right)^{n-1} - \frac{1}{4}(1+\sqrt{2})\epsilon_n^2 3^{n-1}.\end{aligned} \tag{9}$$

Noting

$$\left(\frac{3}{2^k}\right)^{n-1} = \frac{2^k}{3}(2+\sqrt{2})^{k-\log(3)/\log(2)}\epsilon_n^{k-\log(3)/\log(2)}$$

for $k=0,1,2$, gives

$$\text{Area}(G_{\epsilon_n}) = \epsilon_n + \left(\pi + \frac{3+2\sqrt{2}}{4}\right)\epsilon_n^2 + K\epsilon_n^{2-\log 3/\log 2}$$

where K is a constant, equal to $\frac{79+55\sqrt{2}}{12}(2+\sqrt{2})^{-\log 3/\log 2}$. The scaling behavior of $\text{Area}(G_{\epsilon_n})$ as $\epsilon_n \to 0$ is dominated by the smallest power of ϵ_n, which is $2-\log 3/\log 2$. This can be seen by factoring out this power, to obtain

$$\text{Area}(G_{\epsilon_n}) = \left(\epsilon_n^{(\log 3/\log 2)-1} + \left(\pi + \frac{3+2\sqrt{2}}{4}\right)\times\epsilon_n^{\log 3/\log 2} + K\right)\epsilon_n^{2-\log 3/\log 2}.$$

As $\epsilon_n \to 0$, the coefficient of $\epsilon_n^{2-\log(3)/\log(2)}$ goes to K. That is, $\text{Area}(G_{\epsilon_n})$ scales as $\epsilon_n^{2-\log(3)/\log(2)} = \epsilon_n^{2-d}$, where d is the similarity dimension of the gasket G.

An alternative approach applies less generally, but can be considerably simpler. Some fractals are embedded in each of a nested sequence of closed sets, *prefractals*, that are stages in a recursive construction of the fractal. Figure 5 illustrates a sequence of five (gray) prefractals, stages in a recursive construction of the gasket.

An area scaling relationship holds, with the continuous family of ϵ-nbhds replaced by the family of prefractals. For example, denoting by G_k

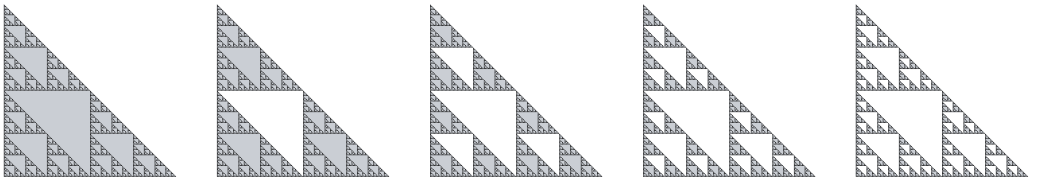

Fig. 5 A sequence of prefractals approximating the gasket.

the kth prefractal of the gasket, so Fig. 5 shows G_0, G_1, G_2, G_3, the scaling hypothesis becomes

$$\text{Area}(G_k) \sim (2^{-k})^{2-d} \tag{10}$$

where 2^{-k} is the side length of the largest filled-in triangle of G_k, the natural length scale of G_k. An easy calcualtion gives $\text{Area}(G_k) = \frac{1}{2}(\frac{3}{4})^k$. Combining this with Eq. (10) yields $\frac{1}{2}(\frac{3}{4})^k = b(2^{-k})^{2-d}$ for some constant b. In the $k \to \infty$ limit this gives $d = \log(3)/\log(2)$.

6. RANDOMNESS AND THE (POSITIVE OR NEGATIVE) TEST DIMENSION; PSEUDO-NEIGHBORHOODS

To begin with a simple illustration, consider the typical intersection of a line A and a point B in the plane. Neglecting the key caveat in the codimension addition rule gives

$$\begin{aligned} 2 - \dim(A \cap B) &= (2 - \dim(A)) + (2 - \dim(B)) \\ &= 3. \end{aligned}$$

This suggests $\dim(A \cap B) = -1$. The absurdity of this result is what motivates the key caveat. How can $\dim(A \cap B) = -1$ be made sensible?

To evaluate the box dimension by the Minkowski-Bouligand approach, calculate how $\text{Area}((A \cap B)_\epsilon)$ scales with ϵ. This cannot be done because typically $A \cap B$ is empty.

One approach to this problem involves two steps. First, replace $(A \cap B)_\epsilon$ with $A_\epsilon \cap B_\epsilon$, called an *$\epsilon$-pseudoneighborhood* (abbreviated hereafer), and test how its measure scales with ϵ. If $A \cap B \neq \emptyset$, the ϵ-nbhd $(A \cap B)_\epsilon$ and the ϵ-pseudonbhd $A_\epsilon \cap B_\epsilon$ exhibit the same scaling relation. This is illustrated in Example 6.1. (Note a similar development is found in Sec. 1.3.3 of Ref. 8. That and the current examples both derive from Ref. 6.)

Example 6.1. Comparing the ϵ-scalings of $(A \cap B)_\epsilon$ and of $A_\epsilon \cap B_\epsilon$.

Let A and B be the rectangles $A = \{(x, y, 0) : 0 \leq x \leq L, -L \leq y \leq L\}$ and $B = \{(x, 0, z) : 0 \leq x \leq L, -L \leq z \leq L\}$. Then $A \cap B = \{(x, 0, 0) : 0 \leq x \leq L\}$ and $(A \cap B)_\epsilon$ consists of a cylinder with radius ϵ and axis L, together with two hemispherical caps. Its volume is

$$\begin{aligned} \text{Volume}((A \cap B)_\epsilon) &= \pi L \epsilon^2 + \frac{4}{3}\pi\epsilon^3 \\ &= \left(\pi L + \frac{4}{3}\pi\epsilon\right)\epsilon^2. \end{aligned} \tag{11}$$

The ϵ-pseudonbhd $A_\epsilon \cap B_\epsilon$ is a parallelopiped with cross-section a square of side length 2ϵ and width L, together with two endcaps, the intersections of the cylinders of radius ϵ along the edges of the rectangles. Its volume is

$$\begin{aligned} \text{Volume}(A_\epsilon \cap B_\epsilon) &= (2\epsilon)^2 L + 2\frac{8}{3}\epsilon^3 \\ &= \left(4L + \frac{16}{3}\epsilon\right)\epsilon^2. \end{aligned} \tag{12}$$

Comparing Eqs. (11) and (12) reveals that the volumes of both $(A \cap B)_\epsilon$ and $A_\epsilon \cap B_\epsilon$ scale as $\epsilon^2 = \epsilon^{3-1}$. That is, the scaling of the ϵ-pseudonbhd detects the dimension of $A \cap B$ in the same way as that of the ϵ-nbhd.

This first step is not sufficient to extend the analysis to empty $A \cap B$: for disjoint compact sets A and B, $A_\epsilon \cap B_\epsilon$ is empty for small enough ϵ. To overcome this problem, the second step consists of sampling at randomly placed points P, computing the expected number $E(N(\epsilon))$ of points P for which P_ϵ intersects both A and B, and calculating how $E(N(\epsilon))$ scales with ϵ. Because this scaling relation is investigated for $\epsilon > 0$, this is called the *pre-asymptotic range*. This calculation is performed for many different placements of A and B, and the results averaged.

That is, the object of study is not the set, which after all is almost surely empty, but rather a process yielding the set. This is precisely in the spirit of the similarity dimension which is defined directly from a process, rather than just as the result of that process.

Example 6.2. Scaling of the ϵ-pseudonbhd of a line and a point in the plane.

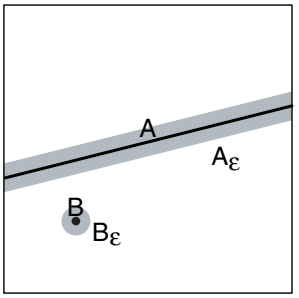

Fig. 6 A line A and a point B in a box of side length L, together with their ϵ-nbhds A_ϵ and B_ϵ.

Consider a line A and a point B both lying in a square S of side length L. Then A_ϵ intersects B_ϵ if $B \in A_{2\epsilon}$. Within S, $A_{2\epsilon}$ occupies an area of $k \cdot L \cdot 4\epsilon$, where k is a factor depending on the slope and placement of A. For horizontal and vertical lines, $k = 1$; for the lines passing through opposite corners of the box, k is slightly less than $\sqrt{2}$. ("Slightly less" because the corners of $A_{2\epsilon}$ lie outside S.) Given A and B placed uniformly randomly within S, the probability that $B \in A_{2\epsilon}$ is $\text{Area}(A_{2\epsilon})/(\text{Area}(S)) = (k \cdot L \cdot 4\epsilon)/L^2$, and so

$$Pr\{A_\epsilon \cap B_\epsilon \neq \emptyset\} = \frac{k \cdot 4\epsilon}{L}.$$

Because B is a point, $N(2\epsilon)$, the minimum number of squares of side length 2ϵ needed to cover $A_\epsilon \cap B_\epsilon$, is at most 1. Note

$$N(2\epsilon) = \begin{cases} 1, & \text{if } A_\epsilon \cap B_\epsilon \neq \emptyset \\ 0, & \text{if } A_\epsilon \cap B_\epsilon = \emptyset \end{cases}. \tag{13}$$

Thus

$$\begin{aligned} E(N(2\epsilon)) &= 0 \cdot Pr\{N(2\epsilon) = 0\} \\ &\quad + 1 \cdot Pr\{N(2\epsilon) = 1\} \\ &= \frac{4k}{L}\epsilon \end{aligned} \tag{14}$$

and consequently the test dimension $D_t(A \cap B)$ can be computed plausibly as

$$D_t(A \cap B) = \lim_{\xi \to 0} \frac{\log(E(N(\xi)))}{\log(1/\xi)} = -1 \tag{15}$$

using $\xi = 2\epsilon$.

Alternately, following Minkowski,

$$E(\text{Area}(A_\epsilon \cap B_\epsilon)) \sim \epsilon^{2-d}. \tag{16}$$

Estimating $E(\text{Area}(A_\epsilon \cap B_\epsilon))$ by $E(N(2\epsilon))(2\epsilon)^2$ and using Eq. (14) shows the area scales as ϵ^3. The result $d = -1$ is recovered by comparing this with Eq. (16).

Example 6.3. Scaling of the ϵ-pseudonbhd of a line and a point in space.

If A and B are a line and a point contained in a cube of side length L in $\mathbb{R}^3$, then except near the edges of the cube, A_ϵ is a cylinder of radius ϵ. Consequently,

$$Pr\{A_\epsilon \cap B_\epsilon \neq \emptyset\} = \frac{k \cdot (2\epsilon)^2 L}{L^3}$$

and as before the average box-counting dimension of $A \cap B$ can be computed plausibly as

$$\lim_{\epsilon \to 0} \frac{\log(E(N(\epsilon)))}{\log(1/\epsilon)} = -2.$$

Or again, following Minkowski, $E(\text{Vol}(A_\epsilon \cap B_\epsilon)) \sim \epsilon^{3-d}$ and estimating the average volume by $E(N(\epsilon))\epsilon^3$, recovering $d = -2$.

This reinforces our intuition that a point has more opportunity to miss a line in $\mathbb{R}^3$ than in $\mathbb{R}^2$.

To help clarify the interpretation, note that here $E(N)$ refers not to a single construction, but to an average over a random ensemble of instances.

7. AN ILLUSTRATION: BIRTH AND DEATH FRACTALS, MANIFEST OR LATENT

In Sec. 5, a sequence of ϵ nbhds was viewed as a process. This is something of a stretch; in many cases, a set indeed is defined as the limit of a sequence of embedded nbhds, but often these are not ϵ-nbhds of the limit. However, the previous approach readily extends to random fractal sets, defined as limits of prefractals (a non-random variant is described at the end of Sec. 5), each of which is a collection of $N(\epsilon)$ cubes of side length ϵ. Generalizing Eq. (15), define the test dimension D_t by

$$D_t = \lim_{\epsilon \to 0} \frac{\log(E(N(\epsilon)))}{\log(1/\epsilon)}. \tag{17}$$

When the limit exists and is negative, as in the Euclidean examples of Sec. 5, it reduces to an approach based on pseudonbhds and both defines and measures the degree of emptiness.

Birth and death processes provide good examples. See Refs. 28 and 29 for general references, and Ch. 23 of Ref. 23 for an application to random fractals. Example 7.1 illustrates the basic concepts of these processes.

Example 7.1. Birth and death in the unit square.

Start with the unit square S and a *survival probability* p_s. Subdivide S into four congruent subsquares, S_0, S_1, S_2, and S_3, and assign to each S_i a probability p_i with $\sum_i p_i = 1$. The subsquare S_i survives if $p_i < p_s$. Subdivide each surviving S_i into four congruent subsquares S_{i0}, S_{i1}, S_{i2}, and S_{i3}, and assign each a probability p_{ij} with $\sum_j p_{ij} = 1$ for the i of each surviving S_i. The subsquare S_{ij} survives if $p_{ij} < p_s$. Continue. Subsquares of side length 2^{-k} have *length k addresses* denoted by the subscript of $S_{i_1 \ldots i_k}$. Using the familiar IFS formalism[29] with transformations

$$T_i(x, y) = \left(\frac{x}{2}, \frac{y}{2}\right) + (a_i, b_i)$$

where $(a_i, b_i) = (0,0), (\frac{1}{2}, 0), (0, \frac{1}{2}), (\frac{1}{2}, \frac{1}{2})$ for $i = 0, 1, 2, 3$, it follows that

$$S_{i_1 i_2 \ldots i_k} = T_{i_1}(T_{i_2}(\cdots T_{i_k}(S)\cdots)).$$

Note the inclusions

$$S_{i_1} \supset S_{i_1 i_2} \supset \cdots \supset S_{i_1 i_2 \ldots i_k}.$$

Associated with each subsquare $S_{i_1 i_2 \ldots i_k}$ is a sequence $\{p_{i_1}, p_{i_1 i_2}, \ldots, p_{i_1 i_2 \ldots i_k}\}$ of probabilities. Now a picture of a canonical fractal dust can be generated by selecting a threshold survival probability p_s and filling the square if

$$\max\{p_{i_1}, p_{i_1 i_2}, \ldots, p_{i_1 i_2 \ldots i_k}\} < p_s.$$

Otherwise, leave the subsquare empty. Figure 7 shows some examples, with p_s decreasing from left to right.

At each level, p_s is the probability that a particular subsquare is occupied. The number, N, of occupied subsquares satisfies

$$\begin{aligned}
&N = 0 \quad \text{with probability } (1 - p_s)^4 \\
&N = 1 \quad \text{with probability } 4(1 - p_s)^3 p_s \\
&N = 2 \quad \text{with probability } 6(1 - p_s)^2 p_s^2 \\
&N = 3 \quad \text{with probability } 4(1 - p_s) p_s^3 \\
&N = 4 \quad \text{with probability } p_s^4.
\end{aligned}$$

By the binomial theorem, the expected number of occupied subsquares of a square is

$$\begin{aligned}
0 \cdot (1 - p_s)^4 + 1 \cdot 4(1 - p_s)^3 p_s + 2 \cdot 6(1 - p_s)^2 p_s^2 \\
+ 3 \cdot 4(1 - p_s) p_s^3 + 4 \cdot p_s^4 = 4p_s
\end{aligned}$$

and the expected number of occupied subsquares of side length 2^{-k} is

$$E(N(2^{-k})) = (4p_s)^k. \tag{18}$$

By Eq. (17) test dimension is

$$D_t = \lim_{k \to \infty} \frac{\log(E(N(2^{-k})))}{\log(2^k)} = 2 + \log_2(p_s). \tag{19}$$

Figure 7 shows instances for which $D_t = 1.6, 1.3, 1.0$, and 0.7, with corresponding $p_s \approx 0.757858$, 0.615572, 0.5, and 0.406126. Anticipating the next section, through each square take an arbitrary linear cut. When $D_t > 1$ the cross-section has a positive probability of being non-empty.

To express this in the standard language of branching processes, observe that each occupied square can have $i = 0$ to 4 occupied subsquares. Denote by $\hat{p}_i$ the probability of having i occupied subsquares. These were computed above, for example, $\hat{p}_1 = 4(1 - p_s)^3 p_s$. Denote by Z_n the number of occupied squares in the nth generation. The extinction theorem proved by Steffensen (page 7 of Ref. 30) shows the probability that nothing survives to the limit is 1 if $f'(1) = E(Z_1) \leq 1$, where $f(s) = \sum_{n=0}^{4} \hat{p}_n s^n$ is the probability generating function. (Note that the number of offspring of a subsquare is $0, \ldots, 4$, so the probability generating function is a finite sum, not an infinite series.) Observe $f'(1) = 4p_s$. When $f'(1) > 1$, the probability that nothing survives to the limit is the unique solution $s = \xi(p_s)$ of $s = f(s) = ((1 - p_s) + p_s s)^4$ in the interval $(0, 1)$. This solution is

$$\xi(p_s) = 1 - \frac{4}{3p_s} - \frac{2^{4/3} p_s^2}{3\rho(p_s)} + \frac{\rho(p_s)}{3 \cdot 2^{1/3} p_s^4} \tag{20}$$

where

$$\rho(p) = ((27 + 3\sqrt{3}\sqrt{27 - 40p + 16p^2})p^8 - 20p^9)^{1/3}.$$

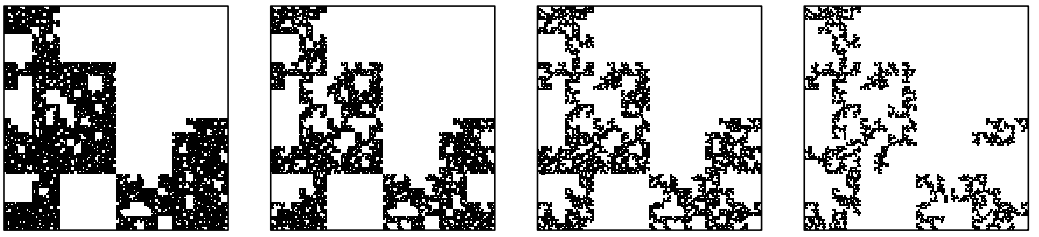

Fig. 7 A sequence of birth and death canonical fractal sets. From left to right the dimensions are $1.6, 1.3, 1.0$, and 0.7.

Note $\xi(\frac{1}{4}) = 1$ and as $p_s \to 0$, $\xi(p_s)$ decreases rapidly to 0.

This dimension calculation also can be done by a method of Lyons.[31] For a branching process with b branches and probability generating function $f(s)$ defining a limit set in the plane, $D_H = \log_{\sqrt{b}}(f'(1))$. In our example, $b = 4$ and $f'(1) = 4p_s$, so we recover the value $\log_2(4p_s)$ for the dimension.

In the construction illustrated by Fig. 7, this suggests two cases: *manifest*, with $D_t > 0$, and *latent*, with $D_t < 0$. In the latent case, almost surely the set is empty and D_t quantifies the process by which the set arrives at being empty. The manifest case has two subcases, corresponding to the limit set being empty and non-empty.

The manifest case. $p_s > \frac{1}{4}$. In this case, Eq. (19) implies $D_t > 0$. Given that $E(Z_1) > 1$, well-known results from the theory of birth and death processes (see pages 12–14 of Ref. 30) can be applied and show that after k stages the number of occupied subsquares takes the form $\Phi E(N(2^{-k}))$, where the prefactor Φ is a random variable that goes to 0 only when nothing survives in the limit. This random prefactor is a consequence of large fluctuations that can occur in early generations. Then a refinement of Eq. (19) is

$$D_t = 2 + \log_2(p_s) + \frac{\log(\Phi)}{\log(2^k)}.$$

As $k \to \infty$, this converges to the value $2 + \log_2(p_s)$ obtained by the simpler calculation.

Note that an empty limit can result even when $E(N) > 1$. Through the process of supersampling, described in Sec. 9, a positive dimension can be associated even with this situation.

The latent case. $p_s < \frac{1}{4}$. In this case, $D_t < 0$. Given that $E(Z_1) \le 1$, from Steffensen's extinction theorem it follows that the limit is almost surely empty. In this case the asymptotic behavior was studied by Kolmogorov and Yaglom, among others. See Sec. 1.8 and later sections (results involving $m < 1$) of Ref. 28. In Secs. 8 and 9 we show other ways in which this analysis can be continued.

8. LIFE BEYOND DEATH I: THE PROCESS OF LINEAR INTERSECTION AND EMBEDDING; CRITICAL EMBEDDING DIMENSION

Carrying out the construction of Example 7.1 applied to subdividing e-dimensional cubes yields random birth and death fractals with

$$D_t = e + \log_2(p_s).$$

Consequently, for a given threshold probability p_s there is a critical embedding dimension

$$e_{\text{crit}} = [\![-\log_2(p_s)]\!] \tag{21}$$

where $[\![x]\!]$ is the smallest integer $\ge x$, so that for all test dimensions $e > e_{\text{crit}}$ the birth and death set has a positive probability of being non-empty and of positive dimension. Then for every p_s, *birth and death fractals with negative test dimension are the intersections between positive test dimension birth and death fractals constructed in* $\mathbb{R}^e$, *with* $e > e_{\text{crit}}$, *and appropriate linear subspaces of* $\mathbb{R}^e$.

Example 8.1. Birth and death on the Sierpinski gasket.

Start with a right isosceles triangle S and replace it with three triangles S_0, S_1, and S_2 determined by $S_i = T_i(S)$, where the T_i are the IFS transformations of Example 7.1. Write $\mathbf{S}_1 = S_0 \cup S_1 \cup S_2$, $\mathbf{S}_2 = S_{00} \cup S_{01} \cup S_{02} \cup S_{10} \cup \cdots \cup S_{22}$, and so on. In the classical language of convergence in the Hausdorff metric (Ref. 24, Ch. 9 of Ref. 1), the $\mathbf{S}_i$ converge to the right isosceles Sierpinski gasket G. Assign probabilities p_i to S_i, subject to the condition $p_1 + p_2 + p_3 = 1$. Each S_i survives if $p_i < p_s$, for some fixed survival probability p_s. Assign probabilities p_{ij} to the surviving S_i, with $p_{i1} + p_{i2} + p_{i3} = 1$. Continue. Preceding as in Example 7.1, the expected number of subtriangles is

$$0 \cdot (1-p_s)^3 + 1 \cdot 2(1-p_s)^2 p_s + 3 \cdot 2(1-p_s)p_s^2 + 3 \cdot p_s^3 = 3p_s$$

and the expected number of occupied triangles of base length 2^{-k} is

$$E(N(2^{-k})) = (3p_s)^k. \tag{22}$$

Call the limit set $G(p_s)$. The test dimension of $G(p_s)$ is

$$D_t = \frac{\log((3p_s)^k)}{\log(2^k)} = \log_2(3) + \log_2(p_s).$$

So $p_s = 2^{D_t - \log_2(3)}$. Note $D_t \le \log_2(3)$, and $D_t \to \log_2(3)$ as $p_s \to 1$. Examples with $D_t = 1.6, 1.3, 1.0$, and 0.7 are seen in Fig. 8. Because $1.6 > \log_2(3) = D_s(\text{Sierpinski gasket})$, the corresponding (formal) $p_s > 1$ and all subtriangles survive. It is no surprise that the left image is the complete gasket.

If L is an arbitrary line crossing the square, then the intersection formula gives

$$D_t(G(p_s) \cap L) = D_t(G(p_s)) - 1.$$

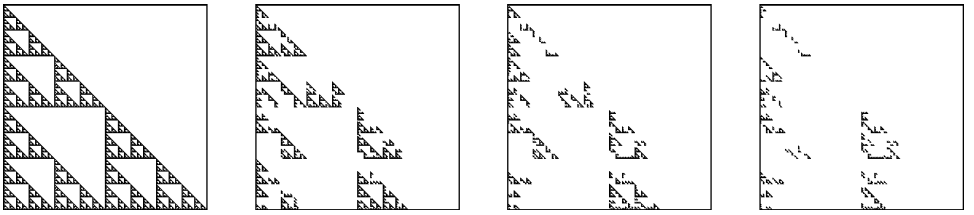

Fig. 8 A sequence of birth and death canonical fractal sets.

So as long as $D_t(G(p_s)) > 1$, there is a positive probability that a linear cut through $G(p_s)$ is non-empty and has positive dimension.

Examples 7.1 and 8.1 have been special in that the IFS are similarities with the same contraction factor. Example 8.2 shows this approach can be applied in a more general setting.

Example 8.2. Birth and death in a fractal with different scaling factors.

Consider the IFS with transformations T_0, T_1, and T_2 of Example 7.1, together with $T_3(x, y) = (x/4, y/4) + (3/4, 3/4)$. Call A the fractal generated by this IFS. The contraction factors are $r_0 = r_1 = r_2 = 1/2$ and $r_3 = 1/4$, so by the Moran Eq. (4) A has dimension $D = \log((3+\sqrt{13})/2)/\log(2)$. See the left image of Fig. 9.

For a given p_s finding the number of occupied squares is more subtle than in the previous examples. Simply finding the number of squares for box-counting requires some thought. Inspecting the left image of Fig. 9 gives

$$N(2^{-1}) = 4 \quad N(2^{-2}) = 13.$$

Noting $T_0(A), T_1(A)$, and $T_2(A)$, the lower left, lower right, and upper left parts of A, are copies of A scaled by $\frac{1}{2}$, and $T_3(A)$, the upper right part of A, is a copy scaled by $\frac{1}{4}$, gives this relation for the number of boxes:

$$N(2^{-(n+1)}) = 3N(2^{-n}) + N(2^{-(n-1)}).$$

To solve this difference equation, suppose $N(2^{-n}) = \lambda^n$. The difference equation becomes $\lambda^{n-1}(\lambda^2 - 3\lambda - 1) = 0$, with solutions $\lambda = (3 \pm \sqrt{13})/2$. Then the general form of $N(2^{-n})$ is

$$N(2^{-n}) = A\left(\frac{3+\sqrt{13}}{2}\right)^n + B\left(\frac{3-\sqrt{13}}{2}\right)^n.$$

Using the initial conditions $N(2^{-1}) = 4$ and $N(2^{-2}) = 13$ to solve for A and B gives

$$N(2^{-n}) = \frac{2(26+7\sqrt{13})}{13(3+\sqrt{13})}\left(\frac{3+\sqrt{13}}{2}\right)^n + \frac{13-5\sqrt{13}}{26}\left(\frac{3-\sqrt{13}}{2}\right)^n.$$

To compute the expected number of occupied subsquares of side length 2^{-n}, use

$$\sum_{k=0}^{n} k\binom{n}{k} p^k(1-p)^{n-k} = np. \tag{23}$$

The proof is a straightforward, if slightly tedious, inductive argument using

$$\binom{n}{k} = \binom{n-1}{k} + \binom{n-1}{k-1}.$$

In Examples 7.1 and 8.1, $N(2^{-(n+1)})$ is expressed as a function of $N(2^{-n})$ establishing a relation between the number of occupied subsquares in one generation and those in the next. This allows the computation of $E(N(2^{-n}))$. Here the generational dependence of $N(2^{-n})$ is more complicated, but it is expressed as a formula of n alone. Recalling the random multiplier is applied in each generation,

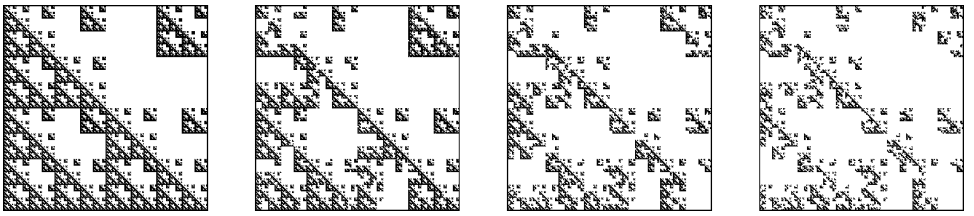

Fig. 9 Another sequence of birth and death canonical fractal sets.

with Eq. (23),

$$E(N(2^{-n})) = \left(\frac{2(26+7\sqrt{13})}{13(3+\sqrt{13})} \left(\frac{3+\sqrt{13}}{2} \right)^n + \frac{13-5\sqrt{13}}{26} \left(\frac{3-\sqrt{13}}{2} \right)^n \right) p_s^n.$$

The test dimension is

$$D_t = \lim_{n\to\infty} \frac{\log(E(N(2^{-n})))}{\log(2^n)} = \log_2((3+\sqrt{13})/2) + \log_2(p_s)$$

so $p_s = 2D_t - \log_2((3+\sqrt{13})/2)$. Note as $p_s \to 1$, D_t approaches the value obtained by the Moran Eq. (4). Figure 9 shows examples of the associated birth and death fractal for several values of p_s. From left to right the dimensions are $D_t = 1.8, 1.5, 1.2$, and 0.9. Note first that $1.8 > (3+\sqrt{13})/2 \approx 1.72368$, so again we find the complete fractal on the left side of the figure.

Also note that when $p_s < 1/(3+\sqrt{13})$ typically (with probability 1) a linear cross-section is empty.

9. LIFE BEYOND DEATH II: THE PROCESS OF SUPERSAMPLING

An alternative to embedding is the notion of supersampling, introduced in Ref. 2. As an illustration, continue with the construction of Example 7.1. To this end, fix $\epsilon = 2^{-k}$ and recall from Eq. (18) that $E(N(2^{-k})) = (4p_s)^k$. Denote by A a set generated by this birth and death process, and by L the line determining the linear cross-section of A. Then

$$E(\text{Area}(A_\epsilon)) \le E(N(\epsilon))\epsilon^2 = (4p_s)^k (2^{-k})^2 = p_s^k$$

and

$$\text{Area}(L_\epsilon) \approx 2\epsilon = 2^{-k+1}.$$

Recalling that the construction takes place within the unit square,

$$Pr\{A_\epsilon \cap L_\epsilon = \emptyset\} \le \frac{\text{Area}(L_\epsilon)}{1 - E(\text{Area}(A_\epsilon))} \le \frac{2^{-k+1}}{1-p_s^k}.$$

By Eq. (19) we see

$$Pr\{A_\epsilon \cap L_\epsilon = \emptyset\} \le 2^{-k+1}/(1-2^{-k(D_t-2)}). \quad (24)$$

For all $p_s < 1$, for sufficiently large k this ratio is less than 1. That is, for some $\eta > 0$,

$$Pr\{A_\epsilon \cap L_\epsilon = \emptyset\} = (1-\eta) \quad (25)$$

For M independent placements of L in the unit square, the probability that each L_ϵ misses A_ϵ is $(1-\eta)^M$, so the probability that for at least one L, $L_\epsilon \cap A_\epsilon \neq \emptyset$ is $1-(1-\eta)^M = \delta$. Using Eqs. (24) and (25), we see

$$\delta \ge 1 - \left(\frac{2^{-k+1}}{1-2^{k(D_t-2)}} \right)^M.$$

The process of taking enough cross-sections to make $L_\epsilon \cap A_\epsilon \neq \emptyset$ likely is called *supersampling*. Note that D_t quantifies the number of samples necessary to obtain a nonempty intersection of ϵ-nbhds. We say D_t measures the degree of supersampling needed to make a latent intersection become manifest.

Finally, note that in the case $p_s > \frac{1}{4}$, the limit still may be empty, with probability $\xi(p_s)$ given by Eq. (20). Then the probability that at least one of M such samples is nonempty is $1-\xi(p_s)^M$. Writing $\xi(p_s) = \delta \ll 1$ gives

$$M = \frac{\log(\delta)}{\log(\xi(p_s))}.$$

Comparing these two expressions for M illuminates the difference between latent and manifest. In the manifest case, the limit may be empty by bad luck; in the latent case, the limit may be nonempty by very, very good luck. The test dimension can be viewed as a quantificaiton of this luck.

10. CONCLUSION

The notion of negative dimension first imposed itself in the context of random multifractal measures. It is indispensable there, both in theory and practice, because it helps to unscramble a variety of forbiddingly complex possibilities. However, sets are far simpler than measures and we found the task of introducing negative dimension to be more manageable in the context of problems concerning sets. We elected to start with the theorem that in three-dimensional space two lines intersect with zero probability. By allowing distinctions finer than empty intersections, negative dimensions open up an infinite range of potentially interesting questions.

To give an example of ideas developed in Ref. 17, where more detail is provided, here we sketch the role of negative dimension in multifractal measures. A clear development of multifractal measures can be found in Chs. 10 and 11 of Ref. 1. Given a measure μ supported on a set A, the local Hölder exponent of μ at $x \in A$ is

$$\alpha(x) = \lim_{r\to 0} \frac{\log(\mu(B(x,r)))}{\log(r)}$$

where $B(x,r)$ is the ball of radius r and center x. The set A is stratified into sets

$$E_\alpha = \{x \in A : \alpha(x) = \alpha\}.$$

The standard derivation of the $f(\alpha)$ curve is

$$f(\alpha) = D_H(E_\alpha).$$

Of course, this does not allow for negative values of $f(\alpha)$. However, $f(\alpha)$ can be defined by generalizing Eq. (7): denoting by $N_\alpha(\epsilon)$ the minuimum number of boxes of side length ϵ needed to cover E_α, multifractality is revealed through a power-law scaling

$$N_\alpha(\epsilon) \sim \epsilon^{-f(\alpha)}.$$

Extending this notion to random multifractals, in Ref. 17 we see how negative values of $f(\alpha)$ can occur, and how to interpret these negative values. In very broad outline, the positive values characterize dimensional properties that are common to all, or almost all, individual sample measures, considered singly. The negative values serve a very different purpose: to help characterize the population of measures and to quantify the likelihood of unlikely values of α.

In the example of random measures on the interval $[0,1]$ with probability distribution Ω, when this distribution is long-tailed, there is a finite critical exponent $q_{\rm crit}$ for which $E(d\mu)^q$ diverges for $q > q_{\rm crit}$ and converges for $q < q_{\rm crit}$. A key theorem states that this exponent depends on negative $f(\alpha)$. This can be interpreted as depending on sets of negative dimension. Because these sets can manifest themselves by the values of traditional quantities that are directly observable, they can be called latent, In Secs. 8 and 9 we saw that latent sets can be made manifest by two procedures: embedding as sections of higher-dimensional non-empty sets, and repeated sampling (supersampling) of finite resolution constructions. Both approaches were suggested by and tested in experimental work in turbulence.[10,11]

ACKNOWLEDGMENTS

Both authors of this paper were partially supported by NSF DMS 0203203. Comments by Rogene Eichler-West were helpful in the preparation of this manuscript. We thank an anonymous referee for useful comments.

REFERENCES

1. K. Falconer, *Techniques in Fractal Geometry* (Wiley, 1997).
2. B. Mandelbrot, A class of multifractal measures with negative (latent) values for the 'dimension' $f(\alpha)$, in *Fractals' Physical Origin and Properties*, ed. L. Pietronero (Plenum, Erice, 1988), pp. 3–29.
3. B. Mandelbrot, Limit lognormal multifractal measures, in *Frontiers of Physics: Landau Memorial Conference*, eds. E. A. Gotsman *et al.*, (Pergamon, 1988), pp. 309–340.
4. B. Mandelbrot, Two meanings of multifractality, and the notion of negative fractal dimension, in *Chaos: Soviet-American Perspectives on Nonlinear Science*, ed. D. Campbell (American Institute of Physics, 1990), pp. 79–90.
5. B. Mandelbrot, Random multifractals: negative dimensions and the resulting limitations of the thermodynamic formalism, *Proc. R. Soc. Lond. A* **434** (1991), 79–88.
6. B. Mandelbrot, Negative dimensions and Hölders, multifractals and their Hölder spectra, and the role of lateral preasymptotics in science, in *Journal of Fourier Analysis and Applications Special Issue*: Orsay, 28 June–3 July, 1993, eds. J.-P. Kahane *et al.* (CRC Press, 1995), pp. 409–432.
7. B. Mandelbrot, Multifractal power-law distributions, other 'anomalies,' and critical dimensions, explained by a simple example, *J. Stat. Phys.* **110** (2003) 739–777.
8. D. Beliaev, Harmonic measures on random fractals, PhD thesis, Royal Institute of Technology, Stockholm (2005).
9. H. Minkowski, Über die Begriffe Länge, Oberfläsche und Volumen, *Jahresber. Deutsch. Math.* **9** (1901) 122–127.
10. A. Chhabra and K. Sreenivasan, Negative dimensions: theory, computation, and experiment, *Phys. Rev. A* **43** (1991) 1114–1117.
11. A. Chhabra and K. Sreenivasan, Scale-invariant multiplier distributions in turbulence, *Phys. Rev. Lett.* **68** (1992) 2762–2765.
12. C. Memeveau and A. Chhabra, Two-point statistics of multifractal measures, *Physica A* **164** (1990) 564–574.
13. C. Meneveau and K. Sreenivasan, The multifractal nature of turbulent energy dissipation, *J. Fluid Mech.* **224** (1991) 429–484.
14. I. Hosokawa, Theory of scale-invariant intermittent measures, *Proc. R. Soc. Lond. A* **453** (1997) 691–710.
15. I. Hosokawa, S.-I. Oide and K. Yamamoto, Trinomial generalized Cantor set model for isotropic turbulence, *J. Phys. Soc. Japan* **65** (1996) 873–875.
16. M. Jensen, G. Paladin and A. Vulpiani, Random fractals, phase transitions, and negative dimension spectra, *Phys. Rev. E* **50** (1994) 4352–4356.
17. B. Mandelbrot and M. Frame, A primer of multifractal measures, of negative test dimensions due

to randomness, and of supersampling to move them from latent to manifest.

18. B. Duplantier, Conformal fractal geometry and boundary quantum gravity, in *Fractal Geometry and Applications: A Jubilee of Benoit Mandelbrot*, Vol. 2, eds. M. Lapidus and M. van Frankenhuijsen (American Mathematical Society, 2004), pp. 365–482.
19. X. Meng, J. Xu and F. Gu, Generalized dimension of the intersection between EEG signals, *Biol. Cybern.* **85** (2001) 313–318.
20. W. Hurewicz and H. Wallman, *Dimension Theory* (Princeton University Press, 1941).
21. B. Mandelbrot, Intermittent turbulence in self-similar cascades: divergence of high moments and dimension of the carrier, *J. Fluid Mech.* **62** (1974) 331–358.
22. J. Lehner, On modular forms of negative dimension, *Michigan Math. J.* **6** (1959) 71–88.
23. B. Mandelbrot, *The Fractal Geometry of Nature* (Freeman, 1982).
24. J. Hutchinson, Fractals and self-similarity, *Indiana Univ. Math. J* **30** (1981) 713–747.
25. M. Lapidus and M. van Frankenhuijsen, *Fractal Geometry, Complex Dimensions and Zeta Functions: Geometry and Spectra of Fractal Strings* (Springer-Verlag, 2006).
26. M. Lapidus and E. Pearse, A tube formula for the Koch snowflake curve, with applications to complex dimensions, *J. Lond. Math. Soc.* **74** (2006) 397–414.
27. S. Winter, Curvature measures and fractals, *Diss. Math.* **453** (2008) 1–68.
28. K. Atreya and P. Ney, *Branching Processes* (Springer, 1972).
29. M. Barnsley, *Fractals Everywhere* (Academic Press, 1988).
30. T. Harris, *The Theory of Branching Processes* (Springer-Verlag, 1963).
31. R. Lyons, Random walks and percolation on trees, *Ann. Prob.* **18** (1990) 931–958.